



Seismic impact between adjacent torsionally coupled buildings

D. Farahani^a, F. Behnamfar^{a,*}, H. Sayyadpour^b, M. Ghandil^a

^a Department of Civil Engineering, Isfahan University of Technology, Esfahan 8415683111, Iran

^b Faculty of Technology and Mining, Yasouj University, Choram 75761-59836, Iran



ARTICLE INFO

Keywords:

Pounding
Torsion
Nonlinear dynamic
Consistent earthquakes
Clear distance

ABSTRACT

The problem of seismic impact between torsionally coupled multi story moment frame buildings is investigated in this paper. Five pairs of adjacent structures spaced at various separation distances are considered. The buildings are 4–10 stories in height. Although a common plan being symmetric with regard to lateral stiffness is considered, a mass eccentricity variable from zero to 30% of the plan dimension is assumed. By three-dimensional modeling of the nonlinear torsional buildings having common story elevations, the seismic pounding happen anywhere along the adjacent buildings edges. Effect of impact and torsional eccentricity are studied by comparison of nonlinear dynamic responses of buildings at different clear distances under 11 consistent earthquakes. The responses include pounding forces at stories, story drifts, story shears and plastic hinge rotations. It is shown that how pounding incidents increase for larger eccentricities and how pounding occurs even at the clear distances prescribed by seismic design codes. The combined effect of torsional eccentricity and pounding results in amplifying the nonlinear response of structure especially for the peripheral frames.

1. Introduction

The seismic pounding can happen between closely spaced adjacent structures during large earthquakes. In such an event, the impact force is applied as a shock on a dynamical system. Such a shock force can alter totally the design responses, as anticipated, for the system under study. Moreover, the local damage sustained by the structural elements under direct impact force, can result in local or global failure in extreme cases.

Because of complexity and existence of many uncertainties in modeling and estimation of pounding, both as an event and as an extra force, it has been the tradition of building codes to set a rule to distance the buildings at an amount to practically eradicate the possibility of impact. Some researchers focused on the adequacy of these prescribed separation distances and possibility of estimating the safe separation distance to avoid pounding. Penzien [1], Lin [2], Jeng et al. [3], Hong et al. [4], Yu et al. [5] and Lopez-Garcia and Soong [6] employed different methods to estimate the required separation distance to avoid seismic pounding between adjacent buildings. Hao and Shen [7] utilized the random vibration procedure to estimate the minimum required separation distance to preclude earthquake-induced pounding between adjacent asymmetric structures. Barros and Khatami [8] investigated the influence of separation distance on pounding between adjacent buildings under near-fault earthquake excitation.

An appropriate model is necessary to simulate pounding effects between adjacent structures and several linear and non-linear models have been proposed so far for the same purpose. Jankowski [9] developed a non-linear viscoelastic model of pounding force to simulate the structural pounding during earthquake. The results showed that their model possessed a better accuracy compared to other linear models but it required more experimental studies to assess the range of the model's parameters for different pounding conditions. Mate et al. [10] studied various pounding elements in the problem of impact of adjacent buildings. They showed that the elements composed of non-linear springs developed smaller impact forces compared with the linear impact elements.

Many attempts have been undertaken by various researchers to investigate the detrimental effects of seismic pounding in the past, especially after the 1985 Mexico City earthquake that exhibited many instances of pounding. The larger volume of the research works in the past 30 years on pounding has been on simple one-dimensional or two-dimensional models of adjacent buildings. However, Jankowski studied the seismic pounding of a 5-story concrete building to a 6-story one using a three dimensional model [11]. Using nonlinear dynamic analysis, it was shown that the shorter building was more affected by the impact phenomenon due to increase of its lateral displacements and plastic strains. In another work by Favvata [12], the pounding of a real RC frame structure with an adjacent shorter and stiffer structure was

* Corresponding author.

E-mail address: farhad@cc.iut.ac.ir (F. Behnamfar).

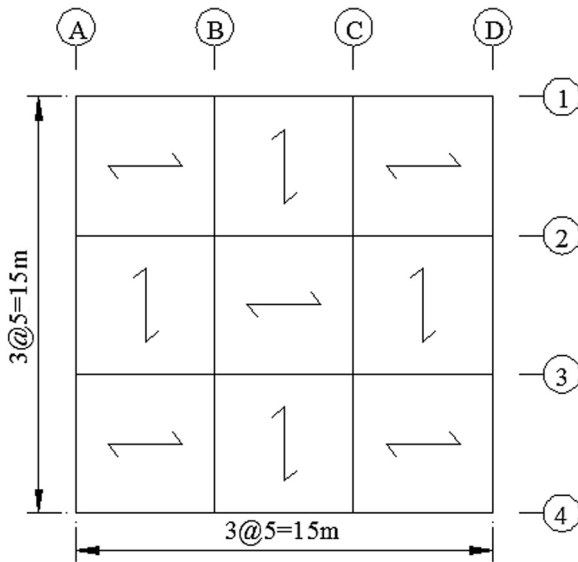


Fig. 1. Typical plan of the buildings.

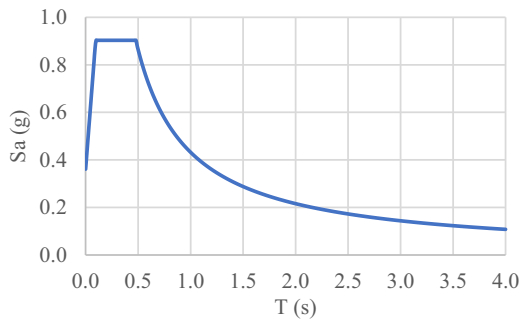


Fig. 2. The design response spectrum.

Table 1
Characteristics of the box columns.

Name	Section dimension (cm)	Section wall thickness (cm)
C1	18	1.75
C2	20	1.75
C3	22	1.75
C4	24	1.75
C5	26	1.75
C6	28	1.75
C7	30	1.75
C8	34	1.75

Table 2
Column sections.

4-Story Building	Story	Axis 1		Axis 2	
		A	B	A	B
4-Story Building	1, 2	C5	C5	C5	C5
	3, 4	C2	C2	C2	C2
	7-Story Building	Story	Axis 1	Axis 2	
7-Story Building	1, 2	A	B	A	B
	3	C5	C5	C5	C5
	4, 5	C3	C4	C4	C4
	6, 7	C1	C1	C1	C1
	10-Story Building	Story	Axis 1	Axis 2	
10-Story Building	1–3	A	B	A	B
	4–6	C7	C8	C7	C8
	7–10	C6	C6	C6	C7

investigated. The results indicated that in all of the examined cases, the external column of the taller building was always in a critical condition due to shear action and high ductility demands.

The pounding phenomenon becomes much more complicated if the effects of other existing parameters, including torsional response, are taken into account. Several research tasks have been devoted to considering simultaneous effects of pounding and torsional coupling [13–18].

Rajaram and Ramancharla [19] evaluated the seismic response of a pair of adjacent single story reinforced concrete (RC) structures with mass eccentricity. They observed greater impact forces at larger clear distances though the number of impacts was reported to be unchanged. The softer building was more influenced by pounding consequences. Fiore and Marano [20] studied simple models of adjacent torsional buildings on rigid bases under seismic impact. They utilized a nonlinear viscoelastic element for transfer of the pounding force. They concluded that the torsional response had a detrimental effect on the number of impacts and lateral displacements of buildings, especially in the lighter and softer structure.

Gong and Hao [21] studied the effects of pounding in single story torsional buildings. To activate torsion, the mass center was displaced relative to the center of stiffness. It was observed that the torsional impact resulted in increase of column shears in stiffer and its reduction in softer buildings. Moreover, pounding increased the torsional response in both buildings, especially in the stiffer one. The building code requirements pertaining the clear distance were deemed not to be adequate to prevent impact in adjacent structures.

The objective of the present study is to investigate the seismic pounding between torsionally coupled adjacent structures. As mentioned in the above related literature, utilizing 3D nonlinear building models for predicting the earthquake-induced pounding between torsionally coupled adjacent buildings remains a research need. Therefore, 3D nonlinear building models are employed for the purpose of the current study. More details are presented in the following sections.

2. Design of the studied buildings

Steel special moment frame buildings being 4, 7, and 10 stories high are investigated. All of the building are common in their plans that is 15 × 15 m with three equal spans in each direction (shown in Fig. 1). The story heights are identically 3.3 m. The fixed-base buildings are considered to be resting on a soft soil (soil type D, ASCE 7–10 [22]) for design purposes. The location of buildings is assumed to have a very high seismicity. The buildings function is residential occupancy. The design acceleration spectrum of the buildings is shown in Fig. 2. The columns and beams are selected to have box and I sections, respectively. The buildings are designed based on AISC360-10 [23]. Characteristics of the designed structural members are shown in Tables 1–3.

The fundamental periods are calculated to be 1.1, 1.96, and 2.33 s for the 4, 7, and 10-story buildings, respectively. It is to be mentioned that when designing the buildings, they are assumed to have no eccentricity (except of the minimum value of the code) to retain the same basis for comparison. Unsymmetry is included later in nonlinear time history analysis by displacing the mass center.

3. Nonlinear modeling

Five pairs of the considered steel moment frame buildings are studied in this paper. Referring to the number of stories, (4, 4), (4, 7), (4, 10), (7, 10), and (10, 10) pairs are investigated. For instance, a (4, 4) pair means a 4-story building adjacent to a 4-story building. The nonlinear modeling of the buildings and the pounding elements between the adjacent structures within OpenSees is mentioned in the following.

Table 3
Beams section properties (Bays in Fig. 1 from left to right or up to down).

Story Axis	4-Story Building			7-Story Building			10-Story Building		
	Bay 1	Bay 2	Bay 3	Bay 1	Bay 2	Bay 3	Bay 1	Bay 2	Bay 3
Axis 1	IPE300	IPE330	IPE300	IPE300	IPE360	IPE300	IPE330	IPE400	IPE330
Axis 2	IPE330	IPE330	IPE330	IPE360	IPE270	IPE360	IPE360	IPE360	IPE360
Axis 3	IPE330	IPE330	IPE330	IPE360	IPE270	IPE360	IPE360	IPE360	IPE360
Axis 4	IPE300	IPE330	IPE300	IPE300	IPE360	IPE300	IPE330	IPE400	IPE330
Axis A	IPE330	IPE300	IPE330	IPE360	IPE270	IPE360	IPE360	IPE360	IPE360
Axis B	IPE330	IPE330	IPE330	IPE360	IPE270	IPE360	IPE360	IPE360	IPE360
Axis C	IPE330	IPE330	IPE330	IPE360	IPE270	IPE360	IPE360	IPE360	IPE360
Axis D	IPE330	IPE300	IPE330	IPE360	IPE270	IPE360	IPE360	IPE360	IPE360

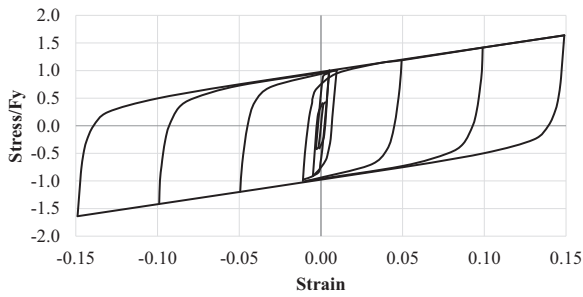


Fig. 3. The Steel02 material [24].

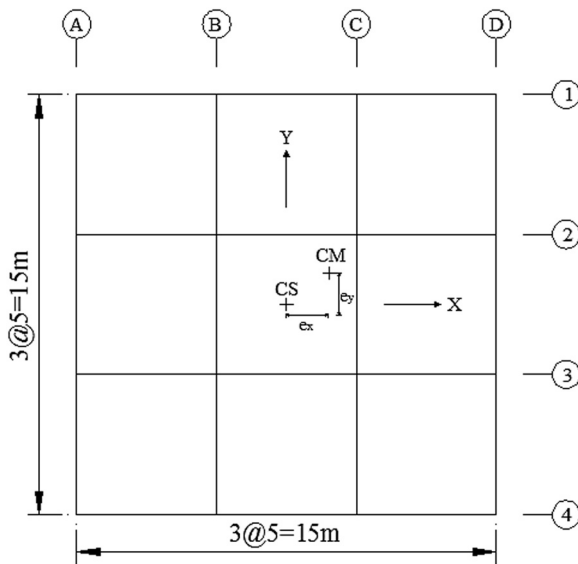


Fig. 4. Eccentricity of the center of mass.

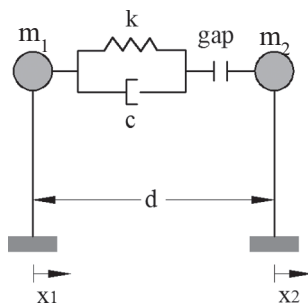


Fig. 5. The linear viscoelastic model for pounding.

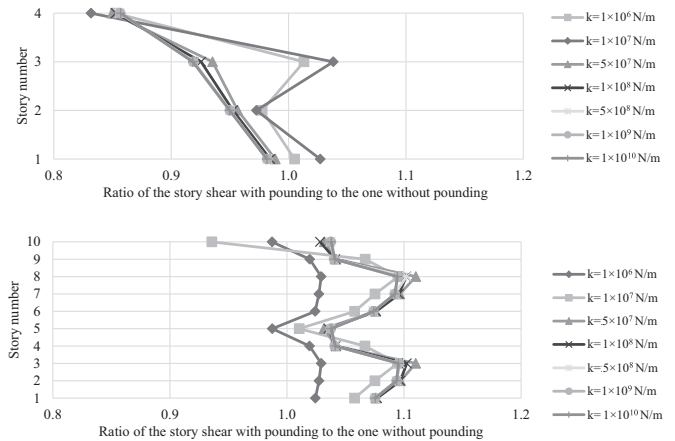


Fig. 6. Convergence analysis for the stiffness of the link element.

Table 4
Width of the separation joint.

Adjacent structures	Width of the separation joint (m)
4, 4	0.19
4, 7	0.25
4, 10	0.18
7, 10	0.33
10, 10	0.38

3.1. Structural members

Out of the available options, including distributed and concentrated plasticity, the latter is selected for modeling of nonlinear behavior in bending in the beams and columns, because of its mutual simplicity and good accuracy. For this purpose, nonlinear moment-rotation hinges are assigned to the end sections of the members, centered at a distance equal to the section depth from the end point of the member. The nonlinear relation is constructed by dividing the section into longitudinal ‘fibers’. The moment-rotation behavior of the section is the resultant of the one-dimensional nonlinear behavior of the fibers, defined by their stress-strain relation. The stress-strain behavior of the steel material of the section can be selected out of the available options of the software. The steel02 material of OpenSees [24] is selected because of its inclusion of strain hardening and the Bauschinger effect and its smooth transition from the elastic to plastic regions that results in a better convergence in nonlinear dynamic analysis. The stress-strain relation of steel02 is shown in Fig. 3.

Table 5
(a) Characteristics of the records. (b) RSN numbers (PEER database code) of the records selected for each building pair.

RSN number	Event	Year	Unscaled PGA (g)		Scale factor
			H1	H2	
57	San Fernando	1971	0.29	0.27	1.54
78	San Fernando	1971	0.11	0.10	1.81
286	Irpinia Italy – 01	1980	0.10	0.08	1.44
755	Loma Prieta	1989	0.15	0.49	1.59
1484	Chi-Chi Taiwan	1999	0.25	0.21	1.43
1616	Duzce Turkey	1999	0.03	0.04	1.43
3747	Cape Mendocino	1992	0.14	0.18	1.44
3750	Cape Mendocino	1992	0.25	0.26	1.45
3753	Landers	1992	0.22	0.20	1.43
3757	Landers	1992	0.14	0.14	1.43
4214	Niigata Japan	2004	0.20	0.23	1.53
4868	Chuetsu-oki	2007	0.32	0.36	1.44
5265	Chuetsu-oki	2007	0.46	0.34	1.53
5663	Iwate	2008	0.50	0.66	1.79
6971	Darfield New Zealand	2010	0.16	0.16	1.44

Order	Adjacent buildings				
	4,4	4,7	4,10	7,10	10,10
1	57	57	57	78	78
2	286	286	286	286	286
3	755	755	755	755	755
4	3750	3750	3750	3747	3747
5	1484	1484	1484	1484	1484
6	1616	1616	1616	1616	1616
7	3753	3757	3757	3757	3757
8	4214	4214	4214	4214	4214
9	4868	5265	5265	5265	5265
10	5663	5663	5663	5663	5663
11	6971	6971	6971	6971	6971

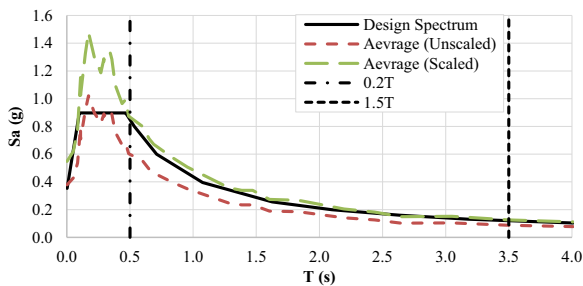


Fig. 7. Scaling of average response spectra for the (4,10) pair of adjacent buildings.

3.2. Effect of torsion

For comparative analysis of this paper, it is imperative to have the same structural members within a symmetric plan and then by making some torsional eccentricity, to evaluate the pounding behavior of the same buildings. This is performed in this study by varying the location of the mass center as observed in Fig. 4. To refrain from introducing too many different cases, equal simultaneous eccentricities are introduced in the x and y directions in the plan. Totally, 5 cases of the eccentricity ratio (i.e. ratio of eccentricity to the plan dimension) are assumed as 0%, 5%, 10%, 20%, and 30%.

3.3. The pounding element

Various mechanical models have been proposed for impact. The linear elastic model, the plastic impact, the Hertz theory of impact, the nonlinear oscillator model, and, the viscous impact model are among them. The Hertz theory of impact was developed by Timoshenko and Goodier [25]. It has been shown that this theory is an appropriate model for a stiff sphere impacting a thick plate at ordinary velocities. For softer materials and higher velocities, the effects of plastic deformations and strain rate must be considered.

The linear viscoelastic model is shown in Fig. 5. It utilizes a dashpot for dissipation of energy during impact. The damping ratio ξ is only a function of the restitution factor e in this model. For $\xi = 0$, a perfectly elastic impact ($e=1$) occurs. The damping coefficient c and the damping ratio ξ are calculated in this model using Eqs. (1) and (2) [26–28]:

$$c_k = 2\xi \sqrt{k \left(\frac{m_1 m_2}{m_1 + m_2} \right)} \tag{1}$$

$$\xi = - \frac{\ln(e)}{\sqrt{\pi^2 + (\ln(e))^2}} \tag{2}$$

where k is the stiffness of the spring, m_1 and m_2 are values of the masses of the two colliding bodies, and e is the restitution factor usually varying between 0.6 and 0.7 [26–28] that is taken to be 0.65 in this study.

Stiffness of the impact spring, that works only in compression, can be estimated from different available relations out of which the two mentioned in the following are more widely used [29]:

$$k = \sum EA/L \tag{3}$$

$$k = \frac{4}{3(k_1 + k_2)} \sqrt{\frac{R_1 R_2}{R_1 + R_2}}; k_i = \frac{1-\nu_i^2}{\pi E_i}; R_i = \sqrt{\frac{3m_i}{4\pi\rho}}; i = 1, 2 \tag{4}$$

According to Eq. (3), the impact stiffness of the same-level floors is considered to be sum of their in-plane stiffnesses that are functions of the elastic modulus E , the section area A , and the length along the impact force L . In Eq. (4), the pounding stiffness depends on properties of the impacting bodies including the Poisson's ratios ν_i , elastic moduli E_i , masses m_i , and the unit masses ρ_i . Stiffness of the link has to be increased until no change is observed in the structural responses. Muthukumar and Desroches [29], and Madani et al. [30] adopted link stiffness values from 1×10^9 to 1×10^{11} N/m for analysis of pounding in multistory buildings.

The adjacent structural models of this study were analyzed under the Elcentro earthquake using a range of stiffness values for the pounding stiffness, being 1.0×10^8 to 1.0×10^{11} N/m. Since in the previous studies, among the response parameters, the story shears have been reported to be most sensitive to the properties of the pounding element, in this study convergency of the same parameter was evaluated using increasing values of the pounding stiffness. It was observed that assuming stiffness values larger than 1.0×10^9 N/m for the pounding element made no change to the response values. A sample of the verification analysis is shown in Fig. 6 where ratio of the maximum story shear with pounding to the one without pounding is shown for different values of the link stiffness. This study results in selecting the pounding element stiffness to be 1.0×10^9 N/m. Occurrence of pounding is simply confirmed when the axial force of the pounding element is nonzero.

Since pounding is not uniform under torsional response and can occur only at a corner, two pounding elements are used with each pounding element located at a corner of the plan adjacent to the nearby

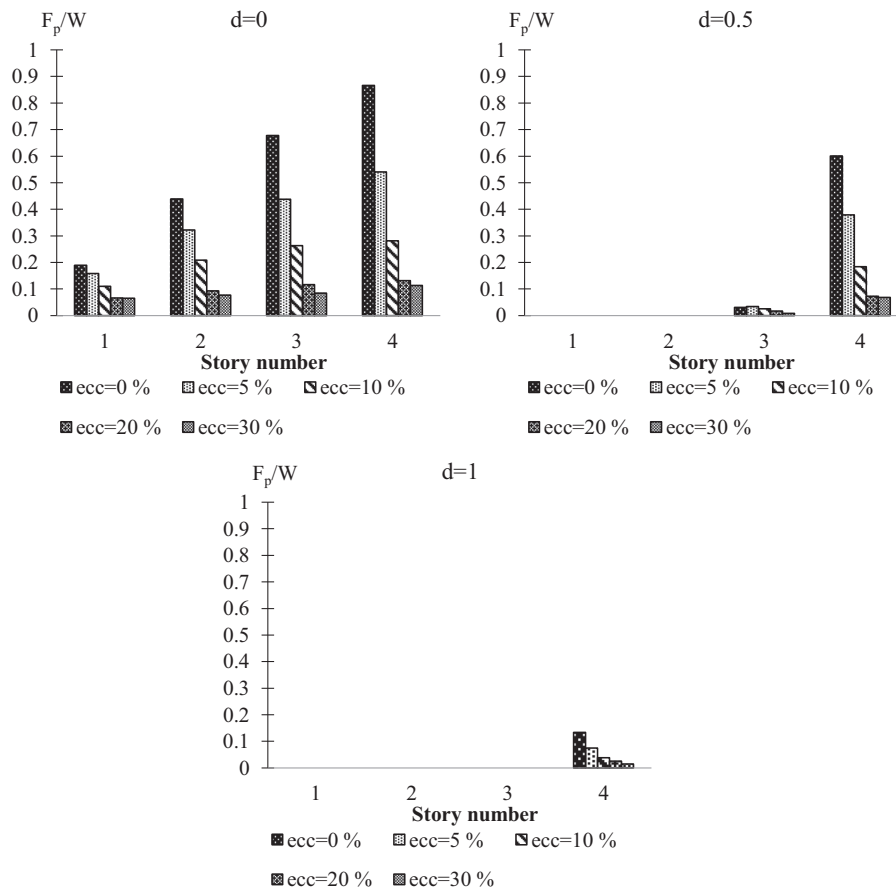


Fig. 8. The normalized pounding force.

Table 6

Number of impacts at the roof of the 4-story building for clear distance of the code.

Record no.	Number of impacts for each eccentricity				
	0%	5%	10%	20%	30%
57	0	0	0	0	0
286	0	0	0	73	90
755	0	4	25	26	49
3750	0	0	0	38	67
1484	15	106	110	114	191
1616	0	0	0	0	0
3757	0	0	0	0	0
4214	0	0	0	0	0
5265	0	0	0	0	0
5663	0	55	80	85	130
6971	0	0	0	0	0

building. According to ASCE7-10, width of the separation joint, δ_{MT} , is calculated using Eq. (5):

$$\delta_{MT} = \sqrt{(\delta_{M1})^2 + (\delta_{M2})^2} \tag{5}$$

where δ_{M1} and δ_{M2} are the design lateral displacements of the adjacent buildings 1 and 2 calculated using Eq. (6):

$$\delta_{Mi} = \frac{C_d \delta_{max}}{I_e} \tag{6}$$

in which δ_{max} is the maximum displacement using the design (linear) spectrum, C_d is the displacement amplification factor (equal to 5.5 for steel special moment frames) and I_e is the importance factor (equal to unity for residential buildings). Table 4 shows the width of the

separation joint calculated using Eqs. (5) and (6), Tables 1–3, and Fig. 1.

In this study, it will be assumed that the adjacent buildings are spaced at 0%, 50% and 100% of the distances required by the code as listed in Table 4 to evaluate its effect on the structural responses.

4. The ground motions

As explained previously, the buildings are assumed to be resting on the soil type D. Therefore, within the database PEER NGA [31], earthquakes recorded on the same soil Type at an intermediate distance of 20–50 km and a magnitude within 6–7.5 Richters are picked up. This resulted in 56 earthquake records as of April 2016. Then, within the records of the same earthquake from various stations, the one having a scale factor nearest to unity is selected. The scale factor is a number that if multiplied by the response spectrum of an earthquake, nowhere between 0.2T and 1.5T it falls below the design spectrum, where T is the fundamental period of the building under study. The above condition results in 11 pairs of ground motion components. For the pair of adjacent buildings, the records having scale factors closer to unity between the two buildings is selected. The unique scale factor of the records selected for each building or building pair is calculated first by constructing an SRSS response spectrum for each pair of horizontal components of the ground motions and then scaling the average of the SRSS spectra for each building or building pair. This process results in Table 5 where the earthquakes selected for each case and their scale factors are collected.

For instance, the average response spectra are shown in Fig. 7 for the (4,10) pair of buildings before and after scaling along with the design spectrum. The two horizontal components of each ground motion are applied to the system concurrently.

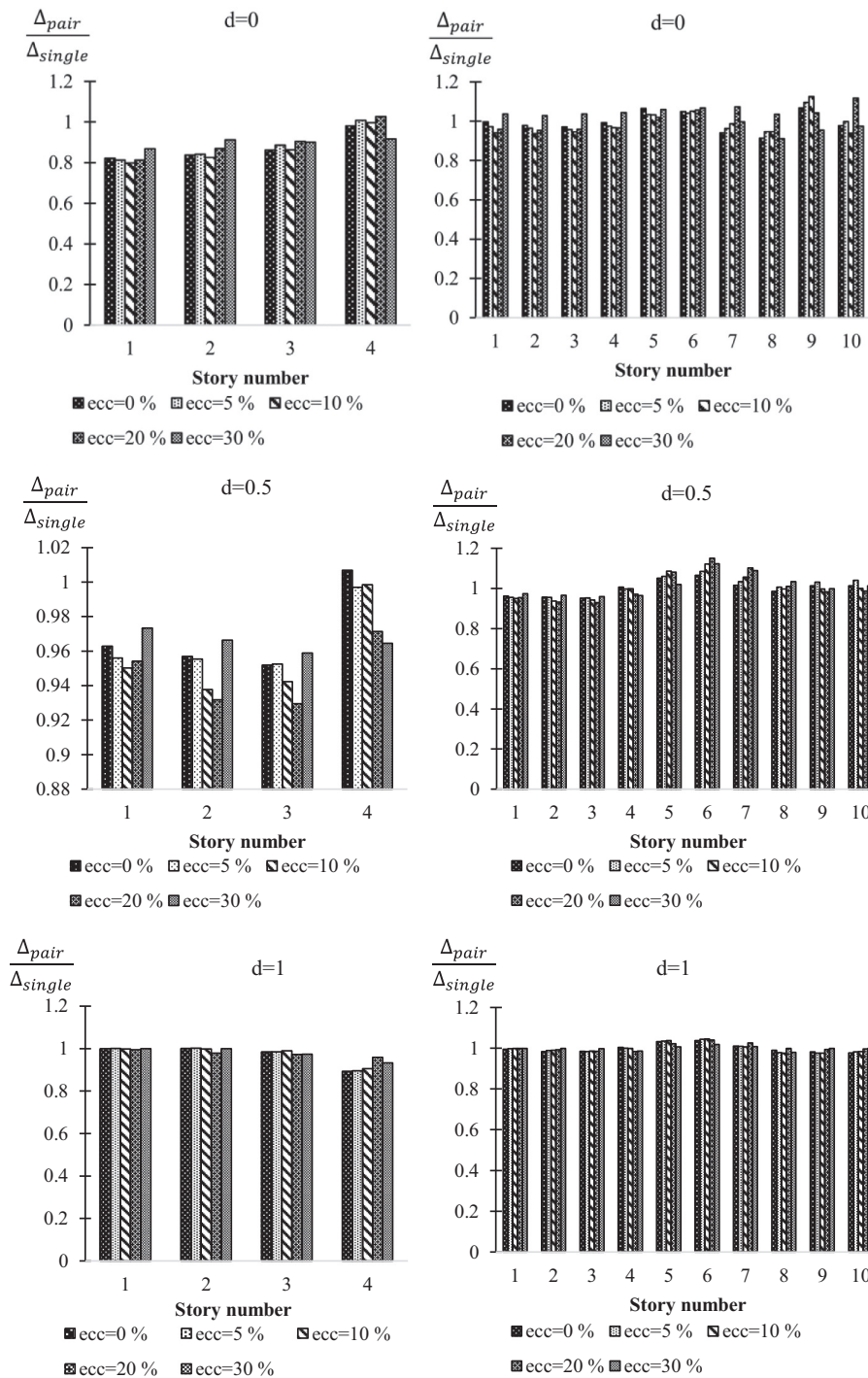


Fig. 9. Distribution of the story drifts normalized to those of the similar single building.

Table 7

Maximum percentages of the story drift reduction (MDR) and increase (MDI) of building pairs with respect to the similar single building drifts.

	Shorter building			Taller building			Shorter building			Taller building		
	Ecc (%)	Story	MDR	Ecc (%)	Story	MDR	Ecc (%)	Story	MDI	Ecc (%)	Story	MDI
4, 4	30	1	3	–	–	–	30	3	14	–	–	–
4, 7	20	1	22	0	5	12	–	–	–	30	7	26
4, 10	10	1	20	30	9	8	20	4	3	20	6	15
7, 10	0	6	20	0	10	14	30	4	7	20	8	25
10, 10	30	10	9	–	–	–	0	1	17	–	–	–

Table 8
Maximum percentages of reduction (DR) and increase (DI) of the story drift ductility demands for the building pairs with respect to the case of a similar single building.

	Shorter building			Taller building			Shorter building			Taller building		
	Ecc. (%)	Story	DR	Ecc. (%)	Story	DR	Ecc. (%)	Story	DI	Ecc. (%)	Story	DI
4, 4	0	1	67	–	–	–	30	3	30	–	–	–
4, 7	30	1	79	0	7	55	–	–	–	30	3	42
4, 10	30	1	80	0	10	75	–	–	–	20	3	20
7, 10	20	7	70	0	10	75	0	3	10	30	3	32
10, 10	0	10	75	–	–	–	30	3	25	–	–	–

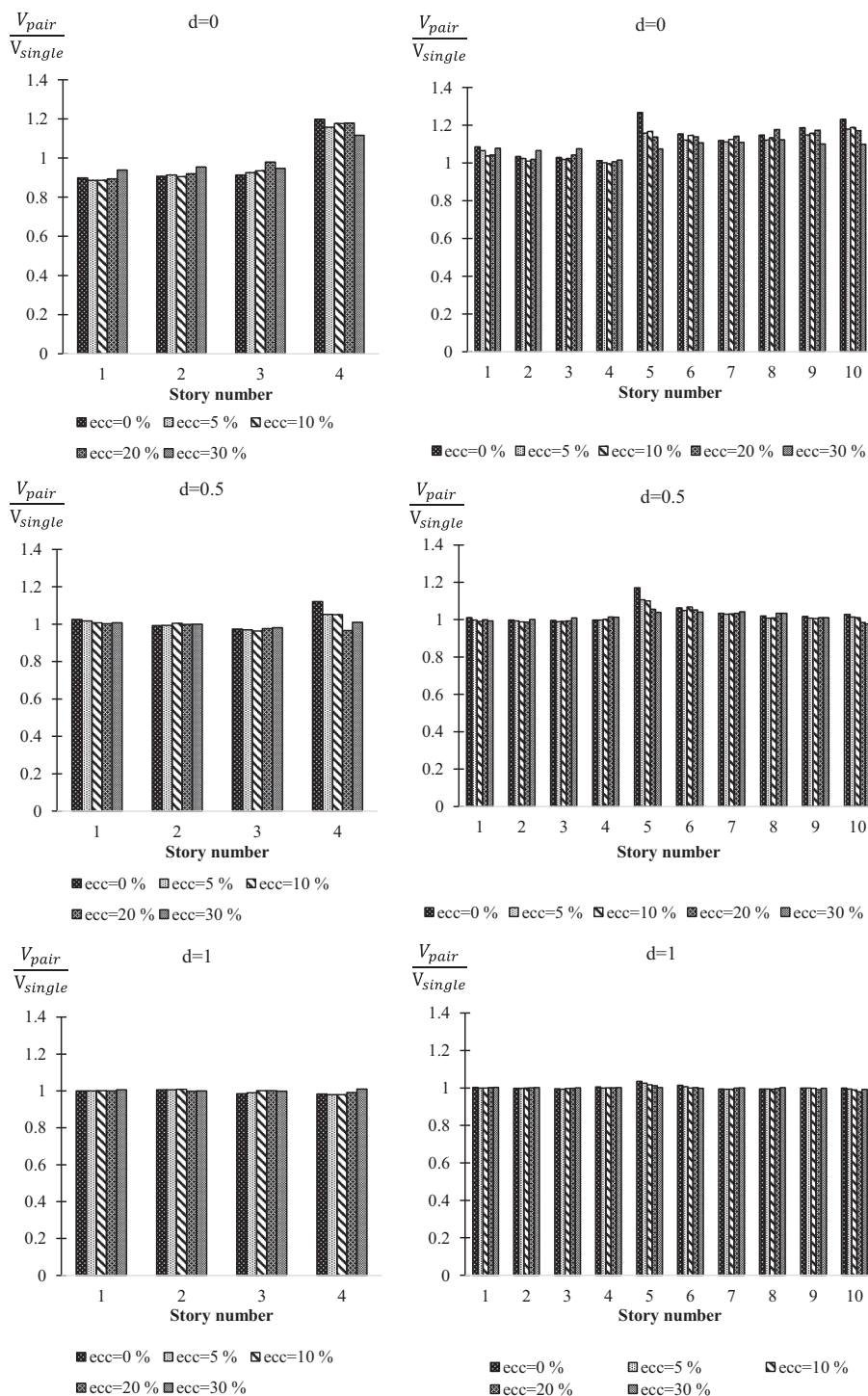


Fig. 10. The story shears normalized to the values without pounding.

Table 9

Maximum percentages of the story shear reduction (SR) and increase (SI) of building pairs with respect to the case of a similar single building.

	Shorter building			Taller building			Shorter building			Taller building		
	Ecc (%)	Story	SR	Ecc (%)	Story	SR	Ecc (%)	Story	SI	Ecc (%)	Story	SI
4, 4	–	–	–	–	–	–	30	4	21	–	–	–
4, 7	20	1	12	–	–	–	0	4	23	0	5	41
4, 10	5	1	11	–	–	–	0	4	19	0	5	26
7, 10	5	2	9	5	7	2	0	7	27	0	8	20
10, 10	–	–	–	–	–	–	30	9	13	–	–	–

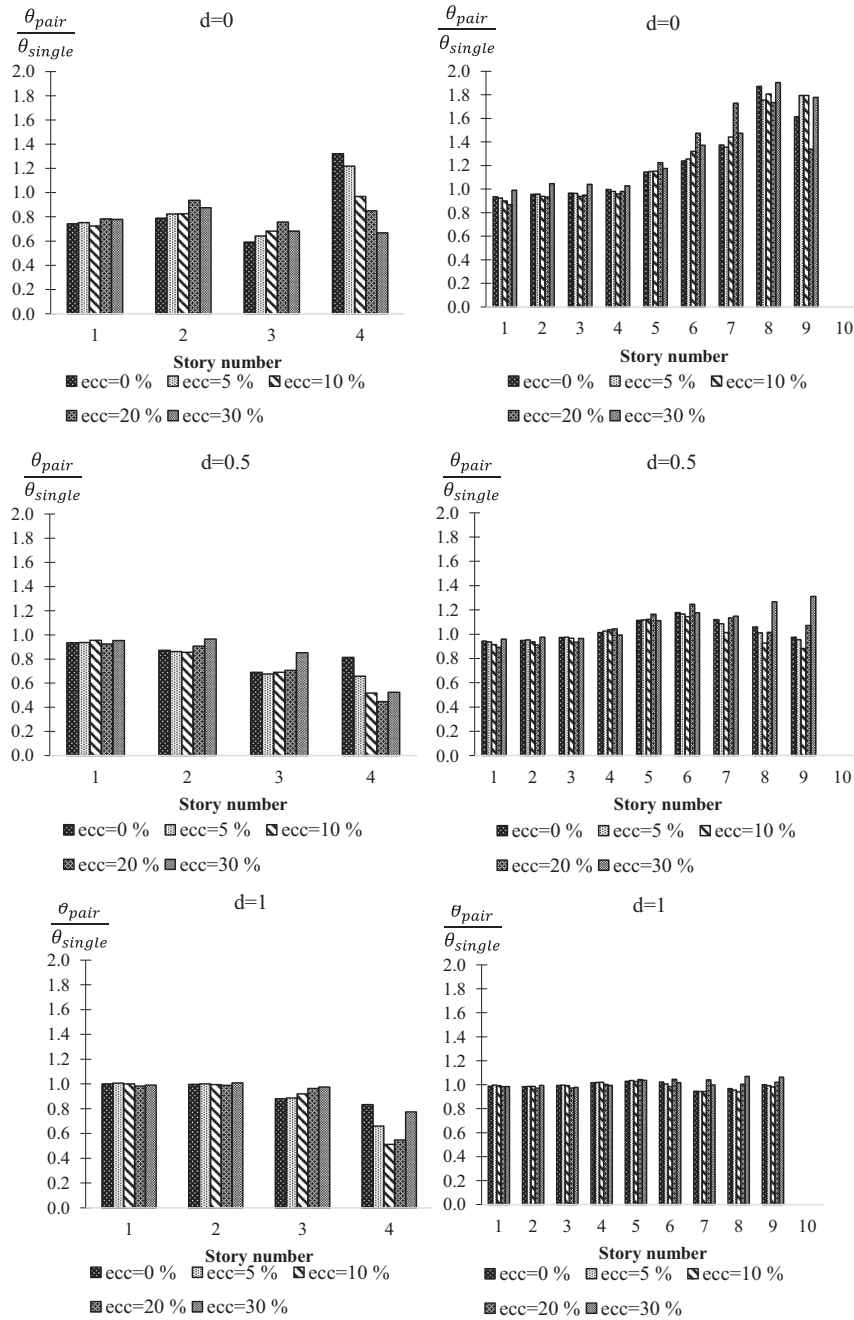


Fig. 11. Resultant plastic hinge rotations of stories of the (4,10) pair normalized to those of the single buildings.

5. Numerical results

5.1. Introduction

As stated in Sections 3, (4,4), (4,7), (4,10), (7,10) and (10,10) pairs of buildings are studied (where the digits refer to the number of stories of adjacent buildings). The mass eccentricity is regarded to be the same in both horizontal directions (see Fig. 4) in both buildings. It is assumed to be 0%, 5%, 10%, 20% and 30% of the plan dimension. The 30% eccentricity is considered both to account for rare cases and to make an interpolation possible. Sign of the eccentricity is obviously of no importance because of the dynamic nature of the analysis. Equality of the eccentricity ratio in both buildings and in both horizontal directions makes a more critical situation. Such an assumption might seem to be conservative but otherwise it would result in too much number of cases

considering also other variables including earthquakes, buildings and clear distance cases. On the other hand, especially for smaller ratios, such eccentricities can often happen because of relocation of the live load or the torsional input of ground motion.

The clear distance between the adjacent buildings is considered to be 0%, 50%, and 100% of the value required by the code (see Section 3.3). Therefore, since the analysis is performed under 11 earthquakes, totally 990 nonlinear time history analyses are implemented for this part of study. The pounding force, drift, shear force, maximum ductility demands, and resultant of the plastic hinge rotations of each story are calculated. The latter quantity is the absolute sum of the plastic hinge rotations of the beams and columns of each story at each moment. The maximum values of the above response parameters are calculated for each earthquake. The average of the maximum values of each quantity is presented in the following. To save space, the comprehensive

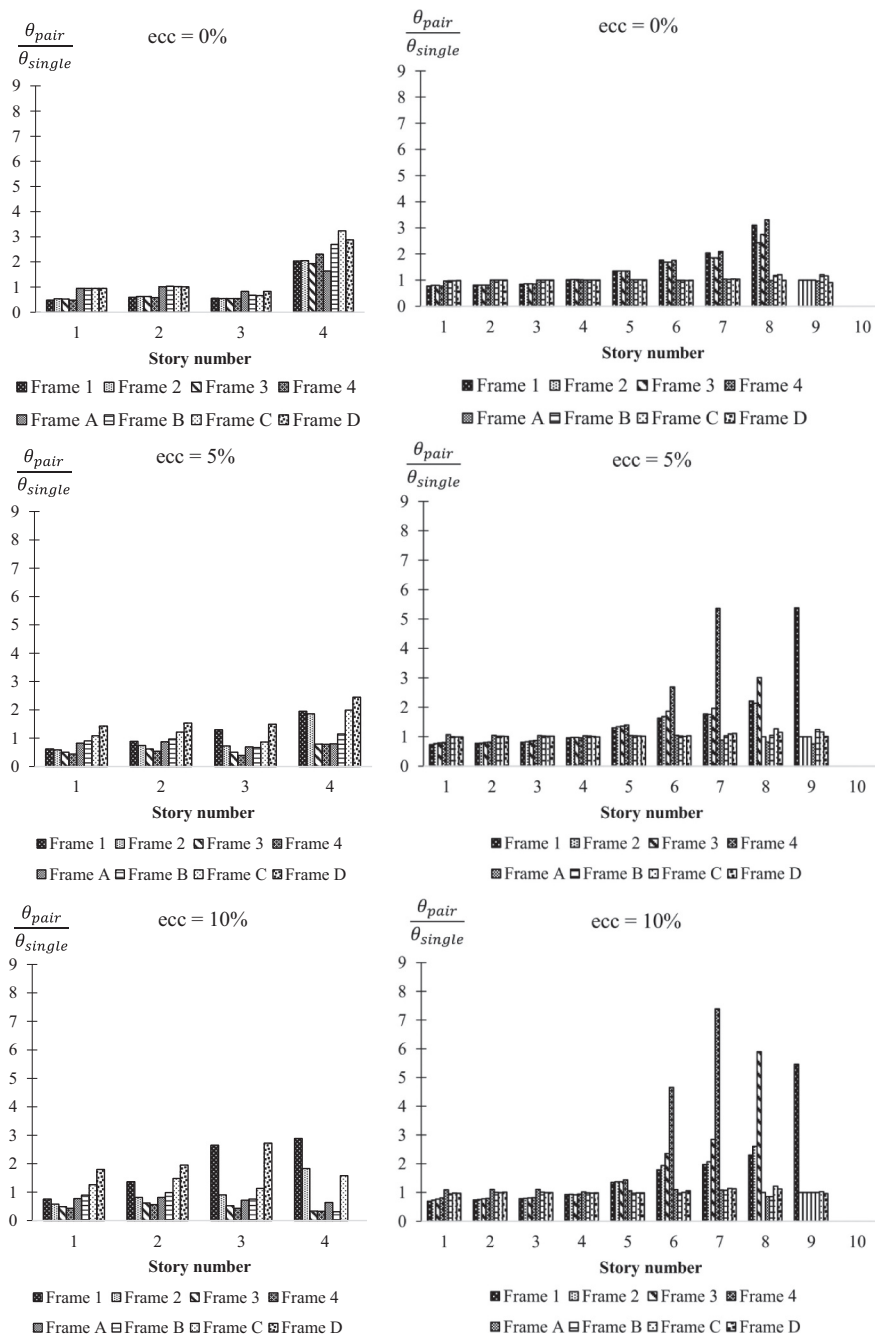


Fig. 12. The PHR ratios for each frame of the (4,10) building pair normalized to those of the similar frame of single buildings for a clear distance ratio of zero.

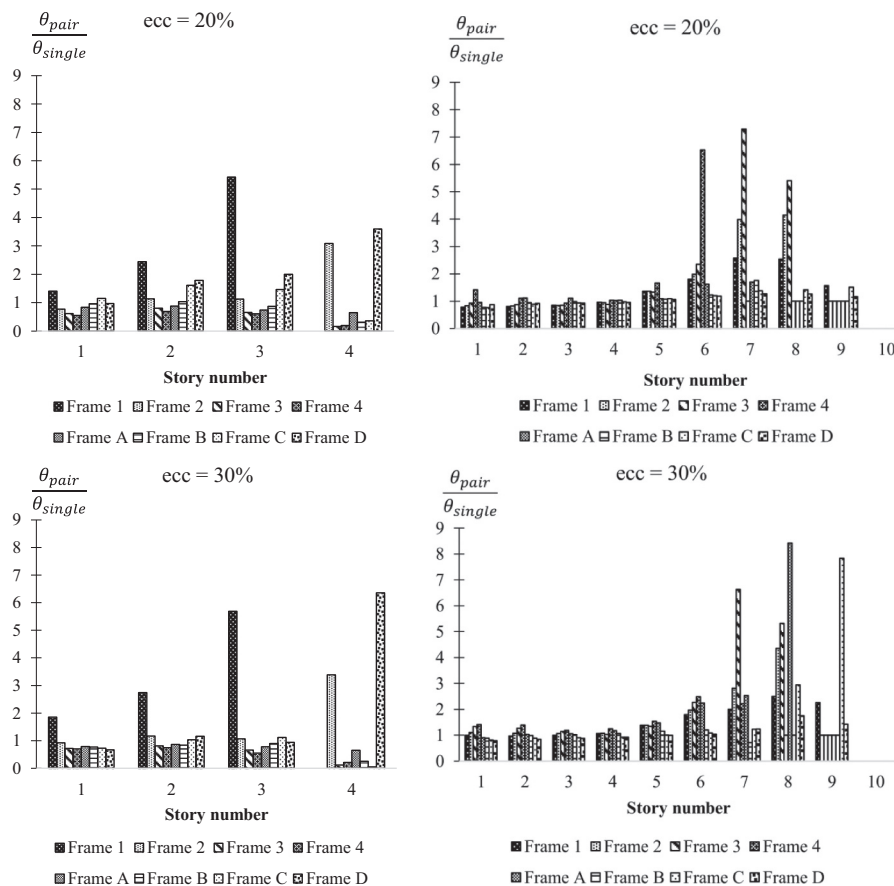


Fig. 12. (continued)

response results are presented only for the (4,10) pair of the buildings. The summarized results of the plastic hinge rotations and ductility demands will be shown also for other pairs. The complete set of the results can be found elsewhere [32]. The analysis results are presented in a normalized form. The pounding force is normalized to the weight of the shorter building and other results are normalized to the corresponding response of the single building case (i.e. the one without pounding).

5.2. The pounding force

Maximum values of the pounding force F_p normalized to the weight of the shorter building (W), are presented in Fig. 8 for different eccentricities and various clear distance ratios d .

It should be noted that without torsion, pounding would occur along the whole width of the floor plans of the adjacent buildings. With torsion, the impact happens only at one corner. In rare cases when the impact is much severe, it can change the direction of rotation of a floor and the impact extends in a certain interval of time to other points of the floor edge. Therefore, pounding does not occur along the whole side of the plan simultaneously with torsion and the pounding force is decreased. Increasing the clear distance between buildings again reduces this force and limits the pounding instances to the upper floors as is clearly observed in Fig. 8. For instance, the pounding force decreases from 0.90 of the building weight for no clear distance and no torsion to about 0.01 for the clear distance of code and a 30% eccentricity. It can be said that pounding is also likely to happen at the clear distance of the code but at a much smaller force. Table 6 shows number of impacts at

the roof of the 4-story building for different values of eccentricity at the clear distance of the code. It is interesting to see that how increasing the eccentricity adds to the number of impacts though at smaller forces.

5.3. The story drifts

The story drifts normalized to the ones of similar single building are shown in Fig. 9

According to Fig. 8, impact occurs in most cases for the above buildings. Therefore, it is anticipated that under the impact incidents, the buildings tend to act as lateral barriers for each other and to lower the difference between lateral motions of contacting stories. But for the stories of the taller building over the shorter one, a ‘splash’ effect occurs that can result in larger drifts. The same behavior is seen in Fig. 9, although variation of the drifts is small on average. The drift ratio decreases as the clear distance increases and this is the direct consequence of the pounding force reduction (see Fig. 8).

Table 7 shows maximum increase and decrease of the story drifts in different cases. As expected, the maximum drift reductions are obtained for the shorter buildings and the maximum drift increases are reported for the taller buildings.

The maximum variations of the story drift ductility demands between the stories of the buildings with respect to the corresponding values of the similar single building are shown in Table 8.

As seen in Table 8, variation of the story drift ductility demands more or less follow the same trend as of the story drifts. In other words, in most cases the reduction ratio is larger for the shorter building. On the opposite, the increase ratio is larger for the taller building.

5.4. The story shears

Distribution of the story shears V normalized to the values without pounding is shown in Fig. 10.

As expected, the story shears overpass the ones without pounding at the stories that experience the most severe effects of the pounding force, i.e. the 4th story in the shorter and the 5th story in the taller building. In the latter case, it happens in the 5th story because lower than that the shorter building acts as a lateral bearing. Also, increase of the story shear should be larger for no eccentricity since in this case, as explained above, the pounding force is larger. This reasoning appears to be valid in most cases in the above figure and in similar figures for other

building pairs. The few cases where increase of eccentricity has increased the story shear correspond to when torsional response has resulted in occurrence of pounding at a story with no pounding in the case of no eccentricity. Moreover, the story shear ratio of the lower and upper stories of the shorter building increased and decreased respectively with increasing the clear distance. It is obviously because of the pounding force effect (see Fig. 8).

Table 9 shows the maximum increase and decrease of the story shears in different cases. As can be observed, maximum variations of the story shears are mostly reported for the small eccentricity ratios and this could be related to the fact that at smaller eccentricities, the pounding happens along the whole side of the plan and therefore, the

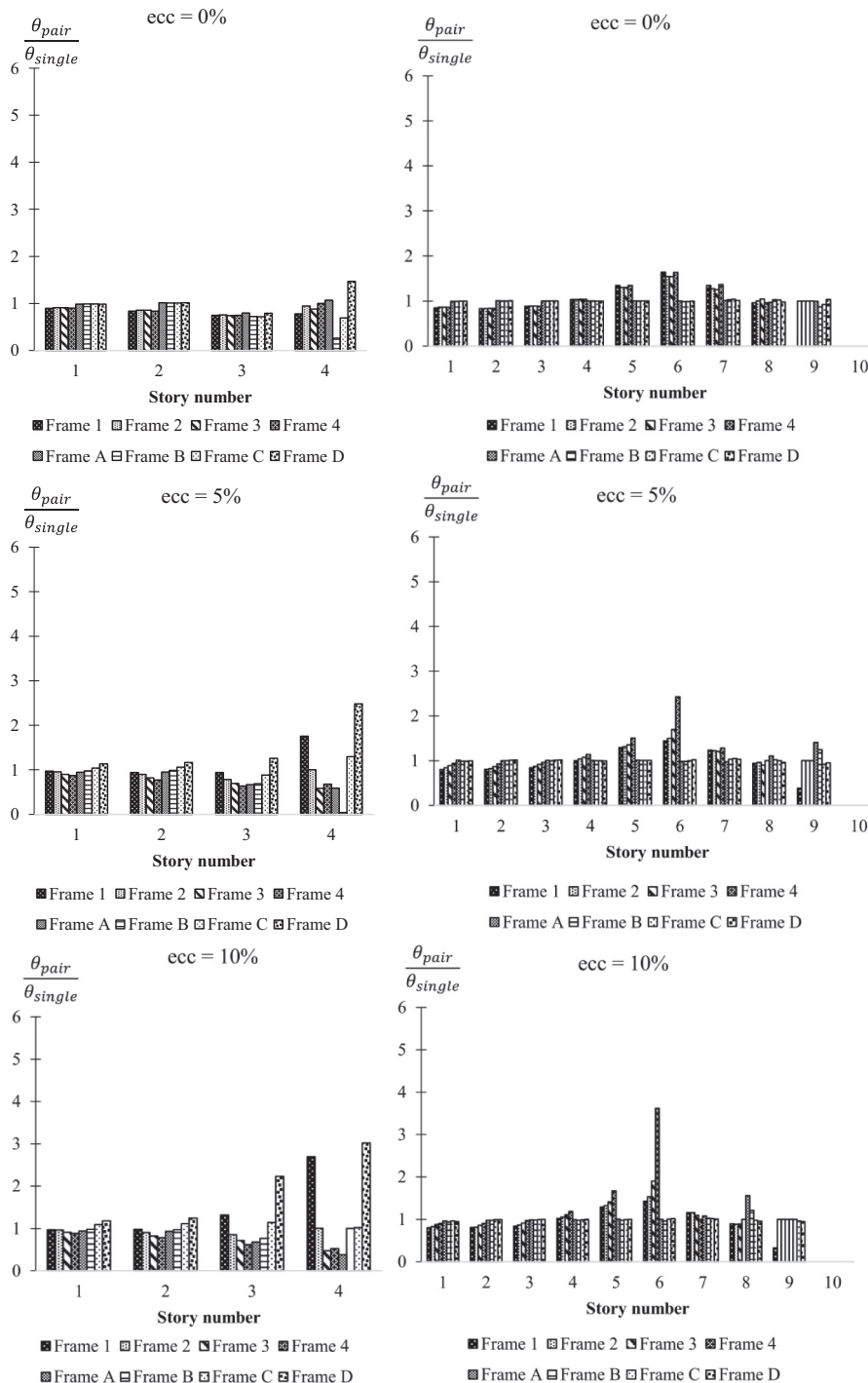


Fig. 13. The PHR ratios for each frame of the (4,10) building pair normalized to those of the similar frame of single buildings for a clear distance ratio of 0.5.

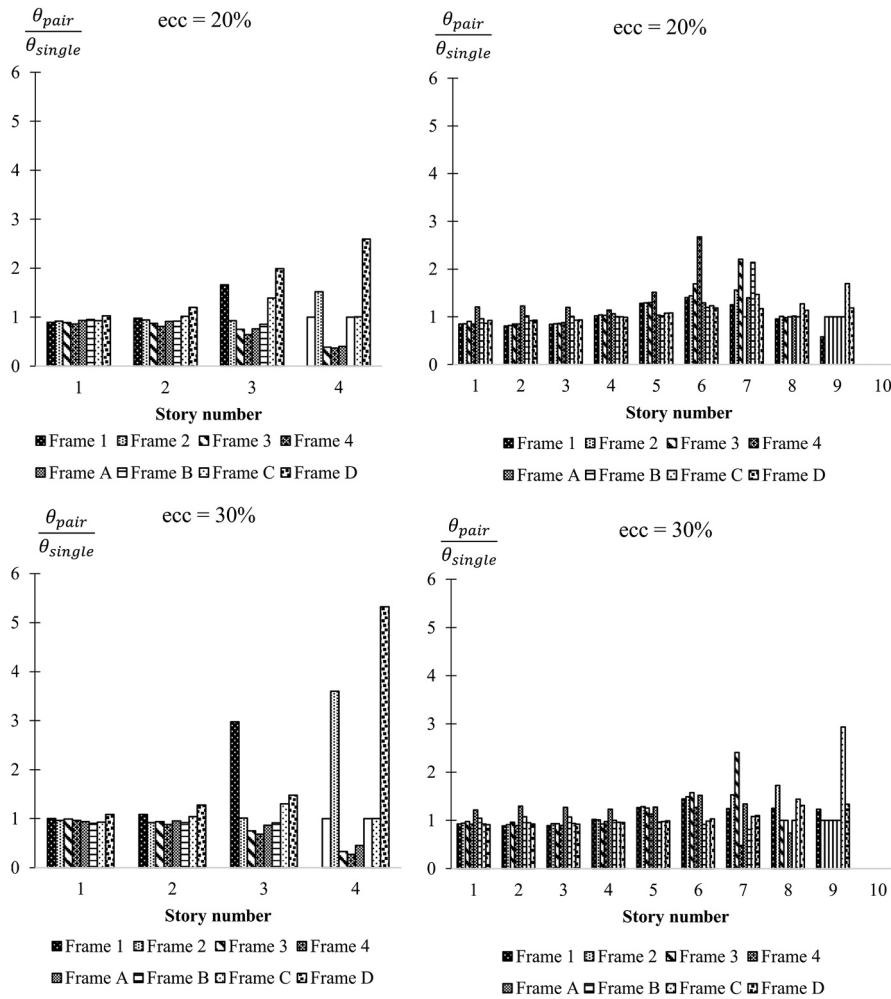


Fig. 13. (continued)

pounding force effects are amplified. The taller building acts like a lateral barrier for the shorter one and this leads to reduction of the story shear in the shorter buildings. However, no remarkable reduction has been recorded for the taller buildings and considerable story shear increases have been obtained for the stories just over the adjacent shorter buildings, because of the sudden lateral stiffness reduction and the so-called splash effect.

5.5. The plastic hinge rotations

Values of the resultants (i.e. maximum absolute sum) of the plastic hinge rotations (PHR's, as defined in Section 5.1) of each story normalized to the similar single building are shown in Fig. 11 for the (4,10) pair case.

A uniform reduction in the PHR is observed with increase of the clear distance. The pounding force should certainly be the cause of this variation as confirmed by resorting to Fig. 8 where larger impact forces are observed at smaller distances. The torsional eccentricity has a non-uniform effect on the plastic response. The PHR's of the stories over the shorter buildings are increased for the same reason mentioned in Section 5.4. It is more serious for the cases with no clear distance and may result in increasing the member damage and possibility of collapse in the upper stories.

To explore the combined effect of torsion and the clear distance, the PHR ratios are separately exhibited in Figs. 12–14 for clear distance ratios of 0, 0.5 and 1 for each frame of the buildings.

It is clearly seen that as the torsional eccentricity increases, the PHR ratios generally increase for those frames of both buildings that are located on the perimeter, as expected. Ratio of the response increase is absolutely maximum for smaller clear distances and can reach values up to 8 for the mentioned frames. But the amplification factor is much smaller for the story as a whole and does not surpass 2. It is also interesting to note that while for clear distance ratios of 0.5 and 1 the PHR ratio is always smaller than unity for the whole stories of the shorter building, it can reach values up to 5 for a certain frame on the perimeter. Therefore, the combined effect of smaller clear distances and larger torsional eccentricities puts the peripheral frames at the worst situation regarding the nonlinear behavior and ductility demand. The larger pounding force at small clear distances should act like an amplification factor for already largely eccentric frames.

Table 10 collects the maximum ratios of PHR increase and decrease in different cases. The largest variations of the story PHR's are observed for the building pairs having unequal heights. On the other hand, increase of the PHR is mostly seen in the cases with higher torsional eccentricity. It shows that torsional eccentricity amplifies effect of the sudden lateral stiffness change of the taller building in its stories located just over the shorter building.

The resultant of the plastic hinge rotations of a story is a more meaningful index for assessing the nonlinear response of that story. Judging the story behavior based on the maximum rotation or ductility demand of just one of its hinges, be it the critical plastic hinge, is extremely conservative.

6. Conclusions

The simultaneous effects of pounding and torsional eccentricity on the nonlinear dynamic responses of pairs of 4, 7 and 10-story steel special moment frame buildings were investigated in this study. Responses including the pounding force, story drift, story shear and resultant of the plastic hinge rotations in each story were calculated under 11 pairs of bi-directional earthquake motions. Through comparison of the average of maxima of each response parameter, the following conclusions were derived for the studied buildings:

1. Pounding of the adjacent buildings can even happen at the clear distance required by the sample seismic design code although with a small amplitude.
2. During the earthquake, the buildings act as lateral barriers for each other and therefore, the difference between lateral motions of contacting stories is reduced. However, upper stories of the taller building may experience larger drifts because of the splash effects.
3. Pounding increases the story shear in the top story of the shorter building and in the story of taller building located just over the shorter one. This effect is more pronounced for smaller eccentricities.

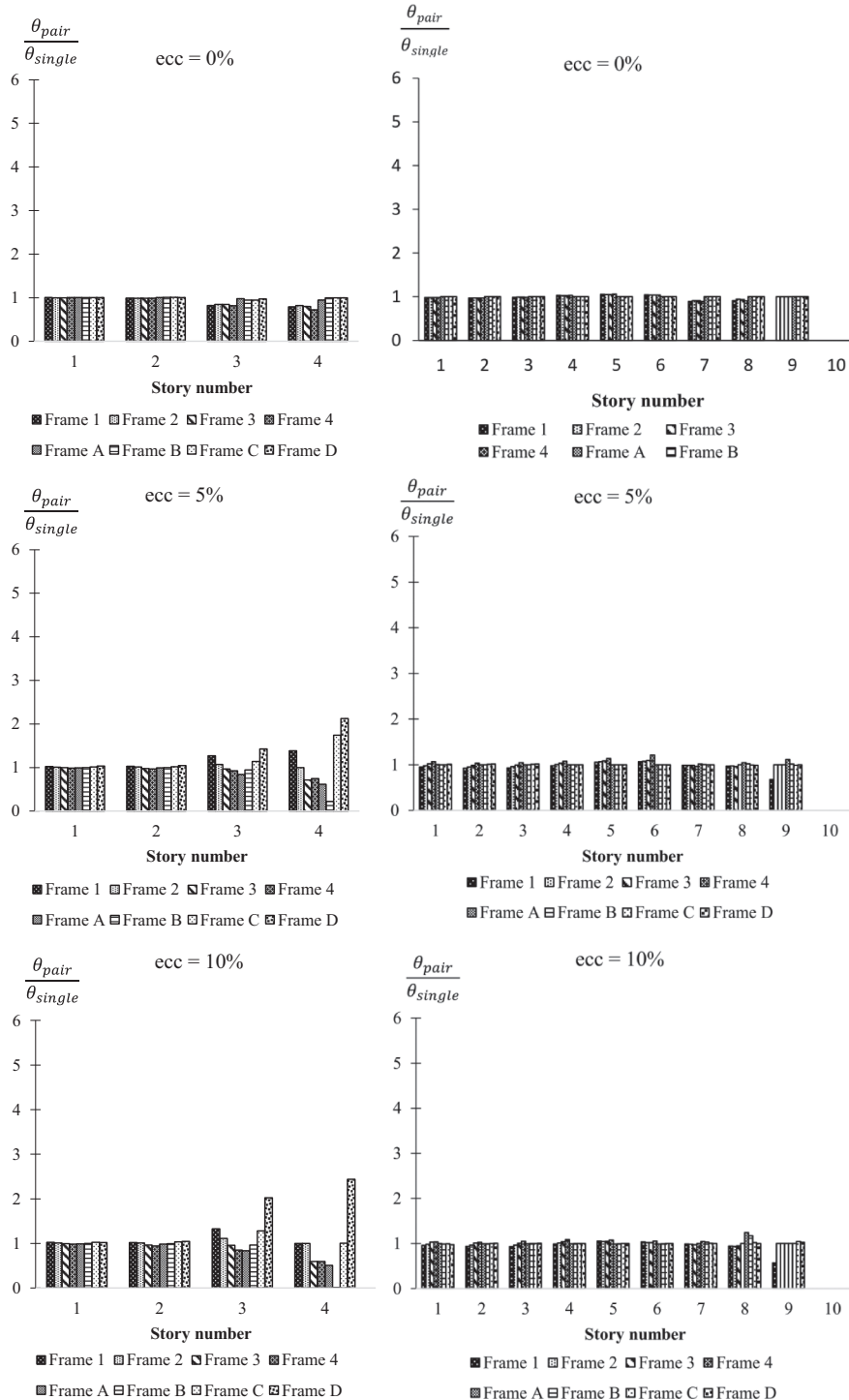


Fig. 14. The PHR ratios for each frame of the (4,10) building pair normalized to those of the similar frames of single buildings for a clear distance ratio of 1.

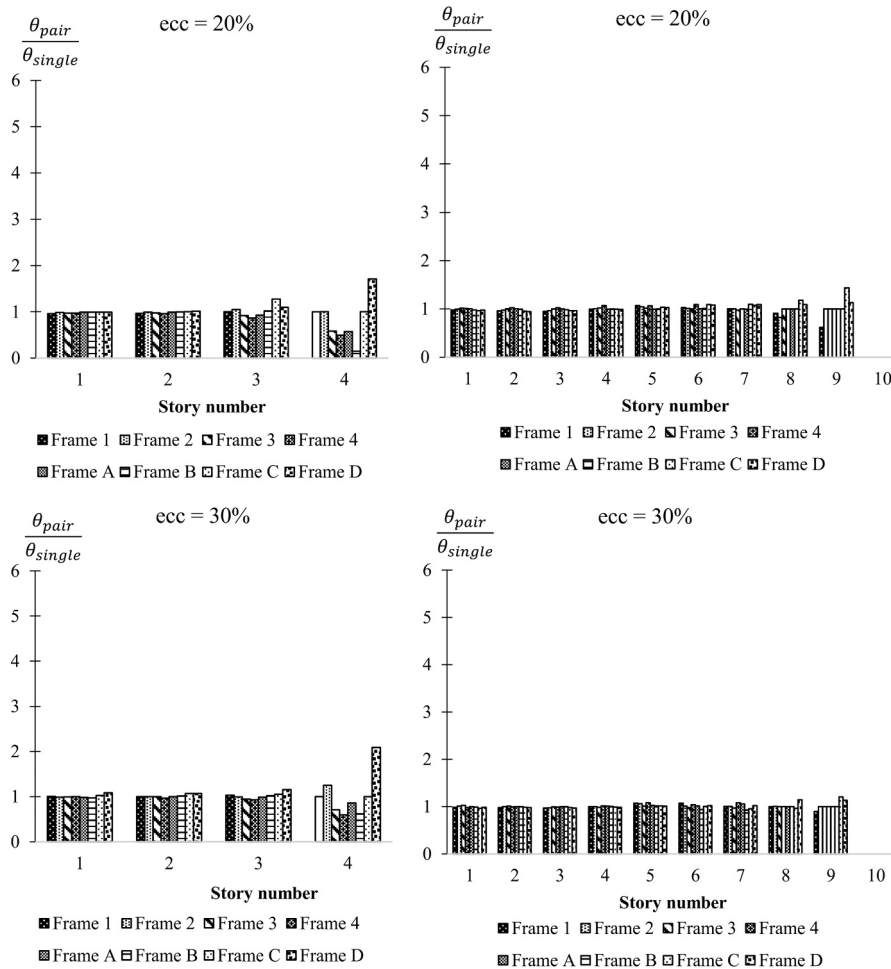


Fig. 14. (continued)

Table 10

Maximum percentages of reduction (PR) and increase (PI) of the story PHR of building pairs normalized to the case of a similar single building.

	Shorter building			Taller building			Shorter building			Taller building		
	Ecc. (%)	Story	PR	Ecc. (%)	Story	PR	Ecc. (%)	Story	PI	Ecc. (%)	Story	PI
4, 4	20	4	27	–	–	–	30	3	37	–	–	–
4, 7	30	4	54	5	4	7	–	–	–	30	6	128
4, 10	20	4	55	20	1	13	0	4	31	30	8	90
7, 10	5	6	49	5	8	14	30	4	22	30	8	93
10, 10	30	7	15	–	–	–	30	8	69	–	–	–

4. Torsional coupling of the seismic response of adjacent buildings makes them to impact at the corners. This phenomenon acts like an amplification factor for the torsional response.
5. Combination of the torsional response and pounding at the corners makes the peripheral frames to be the most critical ones in many cases regarding the nonlinear response and the ductility demand. This is true even at the clear distance required by the code. Such a case needs a special attention.

The present study has been carried out on steel moment frame buildings. Therefore, the conclusions of the study should be looked upon as generally applicable to the steel moment frame buildings up to 10 stories located in highly seismic areas. The future directions of this study should include concrete buildings and buildings with other types of lateral bearing systems resting on flexible bases.

References

- [1] Penzien J. Evaluation of building separation distance required to prevent pounding during strong earthquakes. *Earthq Eng Struct Dyn* 1997;26:849–58.
- [2] LIN J. Separation distance to avoid seismic pounding of adjacent buildings. *Earthq Eng Struct Dyn* 1997;26:395–403.
- [3] Jeng V, Kasai K, Maison BF. A spectral difference method to estimate building separations to avoid pounding. *Earthq Spectra* 1992;8:201–23.
- [4] Hong HP, Wang SS, Hong P. Critical building separation distance in reducing pounding risk under earthquake excitation. *Struct Saf* 2003;25:287–303.
- [5] Yu Z, Liu H, Guo W, Liu Q. A general spectral difference method for calculating the minimum safety distance to avoid the pounding of adjacent structures during earthquakes. *Eng Struct* 2017;150:646–55.
- [6] Lopez-Garcia D, Soong TT. Assessment of the separation necessary to prevent seismic pounding between linear structural systems. *Probab Eng Mech* 2009;24:210–23.
- [7] Hao H, Shen J. Estimation of relative displacement of two adjacent asymmetric structures. *Earthq Eng Struct Dyn* 2001;30:81–96.

- [8] Barros R, Khatami SM. Importance of separation distance on building pounding under near-fault ground motion, using the Iranian earthquake code. In: Proceedings of the 9th Int. Congr. Civ. Eng. Isfahan Univ. Technol. (IUT), Isfahan, Iran; 2012.
- [9] Jankowski R. Non-linear viscoelastic modelling of earthquake-induced structural pounding. *Earthq Eng Struct Dyn* 2005;34:595–611.
- [10] Mate NU, Bakre SV, Jaiswal OR. Seismic pounding of adjacent linear elastic buildings with various contact mechanisms for impact simulation. *Asian J Civ Eng* 2015;16:383–415.
- [11] Jankowski R. Non-linear FEM. analysis of earthquake-induced pounding between the main building and the stairway tower of the Olive View Hospital. *Eng Struct* 2009;31:1851–64.
- [12] Favvata MJ. Minimum required separation gap for adjacent RC frames with potential inter-story seismic pounding. *Eng Struct* 2017;152:643–59.
- [13] Tso WK, Ying H. Additional seismic inelastic deformation caused by structural asymmetry. *Earthq Eng Struct Dyn* 1990;19:243–58.
- [14] Wang LX, Chau KT, Wei XX. Numerical simulations of nonlinear seismic torsional pounding between two single-story structures. *Adv Struct Eng* 2009;12:87–101.
- [15] Tso WK, Ying H. Lateral strength distribution specification to limit additional inelastic deformation of torsionally unbalanced structures. *Eng Struct* 1992;14:263–77.
- [16] Fiore A, Marano GC, Monaco P. Earthquake-induced lateral-torsional pounding between two equal height multi-storey buildings under multiple bi-directional ground motions. *Adv Struct Eng* 2013;16:845–65.
- [17] Ismail M. Elimination of torsion and pounding of isolated asymmetric structures under near-fault ground motions. *Struct Control Heal Monit* 2015;22:1295–324.
- [18] Sołtysik B, Jankowski R. Earthquake-induced pounding between asymmetric steel buildings. *Seism. Behav. Des. Irregul. Complex Civ. Struct. II*. Springer; 2016. p. 255–61.
- [19] Rajaram C, Ramancharla PK. Three dimensional analysis of pounding between adjacent buildings. *J Struct Eng* 2014;41:1–11.
- [20] Fiore A, Marano G. Effect of pounding on the seismic response of two adjacent asymmetric buildings under single uni-directional ground motion. In: Proceedings of the 4th Themat. Conf Comput Meth Struct Dyn Earthq Eng, 2013, p. 3568–79.
- [21] Gong L, Hao H. Analysis of coupled lateral-torsional-pounding responses of one-storey asymmetric adjacent structures subjected to bi-directional ground motions Part I: uniform ground motion input. *Adv Struct Eng* 2005;8:463–79.
- [22] ASCE/SEI 7-10. Minimum design loads for buildings and other structures. Virginia: American Society of Civil Engineers (ASCE); 2010.
- [23] ANSI/AISC 360-10. Specification for structural steel buildings. Am Inst Steel Constr 2010.
- [24] Mazzoni S, McKenna F, Scott MH, Fenves GL. OpenSees command language manual. Berkeley, CA: University of California at Berkeley; 2006.
- [25] Timoshenko S, Goodier JN. Theory of elasticity. 2nd ed. New York: McGraw-Hill Inc.; 1951. <https://doi.org/10.1007/BF00046464>.
- [26] Jankowski R, Mahmoud S. Earthquake-induced structural pounding. Springer; 2015.
- [27] Anagnostopoulos SA. Pounding of buildings in series during earthquakes. *Earthq Eng Struct Dyn* 1988;16:443–56.
- [28] Anagnostopoulos SA. Equivalent viscous damping for modeling inelastic impacts in earthquake pounding problems. *Earthq Eng Struct Dyn* 2004;33:897–902.
- [29] Muthukumar S, DesRoches R. A Hertz contact model with non-linear damping for pounding simulation. *Earthq Eng Struct Dyn* 2006;35:811–28.
- [30] Madani B, Behnamfar F, Riahi HT. Dynamic response of structures subjected to pounding and structure–soil–structure interaction. *Soil Dyn Earthq Eng* 2015;78:46–60.
- [31] PEER strong ground motion database. <<https://ngawest2.berkeley.edu/>>. [Accessed 25 August 2016]; 2016.
- [32] Farahani D. Study on pounding in torsional adjacent buildings considering soil-structure interaction. Isfahan University of Technology; 2017.